# Structural–functional interactions of NS1-BP protein with the splicing and mRNA export machineries for viral and host gene expression

Ke Zhang[a], Guijun Shang[b], Abhilash Padavannil[b], Juan Wang[a], Ramanavelan Sakthivel[a], Xiang Chen[c,d], Min Kim[e], Matthew G. Thompson[f], Adolfo García-Sastre[g,h,i], Kristen W. Lynch[f], Zhijian J. Chen[c,d], Yuh Min Chook[b,1], and Beatriz M. A. Fontoura[a,1]

[a]Department of Cell Biology, University of Texas Southwestern Medical Center, Dallas, TX 75390; [b]Department of Pharmacology, University of Texas Southwestern Medical Center, Dallas, TX 75390; [c]Department of Molecular Biology, University of Texas Southwestern Medical Center, Dallas, TX 75390; [d]Howard Hughes Medical Institute, University of Texas Southwestern Medical Center, Dallas, TX 75390; [e]Department of Bioinformatics, University of Texas Southwestern Medical Center, Dallas, TX 75390; [f]Department of Biochemistry and Biophysics, University of Pennsylvania School of Medicine, Philadelphia, PA 19104; [g]Department of Microbiology, Icahn School of Medicine at Mount Sinai, New York, NY 10029; [h]Global Health and Emerging Pathogens Institute, Icahn School of Medicine at Mount Sinai, New York, NY 10029; and [i]Division of Infectious Diseases, Department of Medicine, Icahn School of Medicine at Mount Sinai, New York, NY 10029

Edited by Thomas E. Shenk, Princeton University, Princeton, NJ, and approved November 13, 2018 (received for review October 23, 2018)

**The influenza virulence factor NS1 protein interacts with the cellular NS1-BP protein to promote splicing and nuclear export of the viral M mRNAs. The viral M1 mRNA encodes the M1 matrix protein and is alternatively spliced into the M2 mRNA, which is translated into the M2 ion channel. These proteins have key functions in viral trafficking and budding. To uncover the NS1-BP structural and functional activities in splicing and nuclear export, we performed proteomics analysis of nuclear NS1-BP binding partners and showed its interaction with constituents of the splicing and mRNA export machineries. NS1-BP BTB domains form dimers in the crystal. Full-length NS1-BP is a dimer in solution and forms at least a dimer in cells. Mutations suggest that dimerization is important for splicing. The central BACK domain of NS1-BP interacts directly with splicing factors such as hnRNP K and PTBP1 and with the viral NS1 protein. The BACK domain is also the site for interactions with mRNA export factor Aly/REF and is required for viral M mRNA nuclear export. The crystal structure of the C-terminal Kelch domain shows that it forms a β-propeller fold, which is required for the splicing function of NS1-BP. This domain interacts with the polymerase II C-terminal domain and SART1, which are involved in recruitment of splicing factors and spliceosome assembly, respectively. NS1-BP functions are not only critical for processing a subset of viral mRNAs but also impact levels and nuclear export of a subset of cellular mRNAs encoding factors involved in metastasis and immunity.**

mRNA export | influenza virus | splicing | NS1 protein | Kelch

Multiple and highly coordinated viral–host interactions with intranuclear pathways dictate the replication of influenza A viruses, which are major human pathogens. The segmented genome of influenza virus, composed of eight single-strand negative-sense RNAs (viral ribonuclear proteins, vRNPs), enters the host cell nucleus for transcription and replication. Two of the viral mRNAs, M and NS mRNAs, undergo alternative splicing to generate critical viral proteins. For example, the M mRNA generates the M1 and M2 proteins involved in viral trafficking and budding. The M1 protein is encoded by the unspliced M1 mRNA, whereas the M2 mRNA is derived by the removal of an intron. The M1 protein is associated with the inner surface of the viral envelope where it appears to interact with the viral glycoproteins and RNPs. The functions of M1 protein include vRNP nuclear export and virion assembly at the plasma membrane. The M2 protein encodes a proton channel that acidifies the viral particle in the endosomes during viral entry, leading to the disruption of M1–vRNP interactions and the release of vRNPs in the cytoplasm, which are subsequently imported into the nucleus (1). M2 also has functions in the late stages of the virus life cycle, including budding (2, 3) and autophagy inhibition (4).

Viral mRNA splicing requires the cellular spliceosome. Most of cellular splicing occurs in the nucleoplasm, where splicing factors are recruited to nascent transcripts through interaction with polymerase II (Pol II). However, there is some evidence that splicing of a subset of mRNAs might be compartmentalized at nuclear speckles (5), which are known to be storage sites of splicing and processing factors (6). We have shown that influenza virus M mRNA is targeted to nuclear speckles for splicing and nuclear export (7). This process requires both viral and cellular proteins. Our findings suggested a model in which the viral protein NS1, a virulence factor of influenza, together with its cellular interacting partner NS1-BP, promotes targeting of the influenza M mRNA to nuclear speckles where heterogeneous nuclear RNP K (hnRNP K), in conjunction with the nuclear speckle assembly factor SON, promotes splicing of M1 mRNA into M2 mRNA through recruitment of the splicing machinery (8). Together with previous findings (9, 10), these results showed

## Significance

A subset of cellular and viral RNAs relies on specific proteins to mediate splicing and nuclear export for proper gene expression. During influenza virus infection, the virulence factor NS1 protein binds the cellular protein NS1-BP to promote splicing and nuclear export of a subset of viral mRNAs that encode critical proteins for viral trafficking and budding. Here we present structures of NS1-BP domains and their functional interactions with components of the splicing and mRNA nuclear export machineries to promote viral gene expression. Additionally, NS1-BP is important for proper expression of a subset of mRNAs involved in metastasis and immunity. These findings reveal basic features of NS1-BP that can be exploited in antiviral therapy and to investigate NS1-BP function in tumorigenesis.

Author contributions: K.Z., G.S., Z.J.C., Y.M.C., and B.M.A.F. designed research; K.Z., G.S., A.P., J.W., R.S., X.C., M.K., and M.G.T. performed research; A.G.-S. contributed new reagents/analytic tools; K.Z., G.S., A.P., J.W., R.S., X.C., M.K., M.G.T., A.G.-S., K.W.L., Z.J.C., Y.M.C., and B.M.A.F. analyzed data; and K.W.L., Y.M.C., and B.M.A.F. wrote the paper.

The authors declare no conflict of interest.

This article is a PNAS Direct Submission.

Published under the PNAS license.

Data deposition: The atomic coordinates reported in this paper have been deposited in the Protein Data Bank, www.wwpdb.org (PDB ID code 6N34 for BTB domain and 6N3H for Kelch domain).

[1]To whom correspondence may be addressed. Email: Yuhmin.Chook@utsouthwestern.edu or Beatriz.Fontoura@UTSouthwestern.edu.

This article contains supporting information online at www.pnas.org/lookup/suppl/doi:10.1073/pnas.1818012115/-/DCSupplemental.

spatial and temporal regulation of M2 expression, which is likely important to prevent premature expression of an ion channel that could be detrimental to the host cell during the early stages of virus replication. In addition, M2 expression likely should be coordinated with budding for effective production of infectious viral particles.

While the core components of the spliceosome have been defined, regulatory factors of this key machinery for gene expression have not been fully explored. The spliceosome is an enzymatic complex composed of five small nuclear RNPs (snRNPs): U1, U2, U4, U5, and U6 (11). Additional factors interact with these snRNPs to regulate the different stages of the splicing cycle. In the case of influenza virus M1 mRNA, we show that the cellular protein NS1-BP interacts with the cellular RNA-binding protein hnRNP K to promote splicing of the viral M1 mRNA. NS1-BP belongs to the Kelch family of proteins. It has a BTB [broad-complex, tramtrack, and bric-a-brac; also known as a "POZ" (Pox virus and zinc finger)] domain at its N terminus, followed by a BACK domain and a C-terminal Kelch domain (Fig. 1*A*). Many characterized BTB domains are dimers (12); the central BACK domains of Kelch proteins contain HEAT repeats that are possibly flexible (13) and bind various proteins; and the C-terminal Kelch domain contains Kelch repeats that form β-propellers and can serve as protein interaction surfaces. The Kelch family of proteins is involved in diverse functions (14). While there are only a few reports on NS1-BP function, they indicate multifunctionality. NS1-BP is localized in the nucleus and in the cytoplasm and is involved in splicing (7, 9, 15), c-myc transcription regulation (16), signal transduction (17), stabilization of actin filaments (18), and protein stability (19). Understanding the players and molecular mechanisms involved in these processes is critical to elucidate how NS1-BP and its interacting partner hnRNP K impact influenza virus replication (7, 9) and cancer metastasis (19, 20). In this study, we identified the NS1-BP nuclear interactome and defined the structural and functional relationship of NS1-BP responsible for its role in splicing and mRNA nuclear export.

## Results

**NS1-BP Interacts with Splicing and mRNA Export Factors.** To dissect the function of NS1-BP in splicing, we first sought to identify interacting partners of NS1-BP in the nucleus. Nuclear extracts from cells stably expressing 3×Flag-NS1-BP, 3×Flag-NS1-BP (BTB-BACK), or 3×Flag (control) were subjected to immunoprecipitation followed by mass spectrometry analysis (*SI Appendix*, Table S1). We have previously shown, in total-cell extracts, that endogenous NS1-BP interacts with hnRNP K and the Pol II C-terminal domain (CTD) (9). We have now identified a subset of splicing factors as interacting partners of NS1-BP including PTBP1 (polypyrimidine tract binding protein 1), U1A (also called "Mud1" or "SNRPA"), and SART1. PTBP1 is a splicing repressor (21). U1A interacts with U1 snRNA, which binds the 5′ splice site of precursor mRNAs constituting the first steps of the splicing reaction (22). SART1 (or Snu66) is a constituent of the U4/U6-U5 triple snRNP (trisnRNP) and has a role in spliceosome activation (22). These interactions were confirmed by immunoprecipitation followed by Western blot (Fig. 1*B*). The splicing factor LSm-8, which also interacts with U4/U6, did not bind NS1-BP (Fig. 1*B*), further indicating the interaction of NS1-BP with a subset of splicing factors. The interactions of splicing factors with NS1-BP were further corroborated in a pull-down assay with purified GST-NS1-BP and cell extracts (Fig. 1*C*). Additionally, NS1-BP interacts with the mRNA export factor Aly/REF (Fig. 1 *B* and *C*), which is known to bind spliceosomes at the late steps of the splicing reaction and links splicing to mRNA nuclear export (23).

Since NS1-BP interacts with factors that bind the spliceosome at different stages of the splicing reaction, we tested whether NS1-BP differentially coeluted with its interacting partners. We performed size-exclusion chromatography of nuclear extracts and followed the elution profiles of NS1-BP and its interacting partners by Western blot. As shown in Fig. 1*D*, most of the NS1-BP protein eluted as a dimer at ∼140 kDa. However, other pools of NS1-BP were also found at higher molecular mass fractions (from 440 kDa to 669 kDa and above) where specific bindings partners coeluted at different positions. This pattern suggests the formation of prespliceosome and spliceosome complexes between NS1-BP and splicing factors. Fraction 11 contains NS1-BP, U1A, and SART1, whereas fractions 9.5 and 10 likely contain the high molecular mass spliceosome where the expected splicing factors and the mRNA export factor Aly/REF coeluted. As mentioned above, Aly/REF interacts with the spliceosome to link splicing to mRNA nuclear export (23). The differences in U1A mobility observed between fractions 9.5 and 11 are likely due to differential phosphorylation (24). Taken together, a pool of NS1-BP binds splicing factors, and the mRNA export factor Aly/REF, and NS1-BP probably associates with prespliceosome and spliceosome complexes.

**Dimerization of NS1-BP via Its BTB Domain Is Required for Splicing.** To understand the mode of action of NS1-BP on splicing, we determined the crystal structure of its BTB domain to 2.8-Å resolution (Fig. 2*A* and *SI Appendix*, Table S2). The NS1-BP BTB forms a homodimer in the crystal (Fig. 2*A*). The NS1-BP BTB homodimer is comprised of a group of α-helices that are flanked by four short β-sheets. The structure is very similar to those of many other BTB domains in the Protein Data Bank (PDB), such as the BTB domains from the LRF/ZBTB7 transcriptional regulator (PDB ID code: 2NN2; rmsd ∼1.33 Å), KLHL11 (PDB ID code: 3I3N; rmsd 1.213 Å), and BCL6 (PDB ID code: 4CP3; rmsd 1.354 Å) (25–27). All four BTB domains have extensive dimer interfaces: The NS1-BP BTB buries 1,804 $Å^2$, 29% of the monomer surface; the LRF/ZBTB7 BTB buries 1,620 $Å^2$, 28% of the monomer surface; the KLHL11 BTB buries 2,510 $Å^2$, 34% of the monomer surface; and the BCL6 BTB buries 2,030 $Å^2$, 30% of the monomer surface. Analytical ultracentrifugation analyses of full-length NS1-BP show the protein to be a dimer in solution (Fig. 2*B*), consistent with the BTB homodimer observed in the crystal (Fig. 2*A*). This is also consistent with size-exclusion chromatography data suggesting a possibly dimeric purified NS1-BP (*SI Appendix*, Fig. S1*A*) and a possibly dimeric NS1-BP in nuclear extract (Fig. 1*D*). To further test the possibility that NS1-BP interacts with itself in cells, Flag-NS1-BP and Myc-NS1-BP were cotransfected into cells and immunoprecipitated with anti-Flag antibody. Flag-NS1-BP coprecipitated with Myc-NS1-BP, indicating that NS1-BP is at least a dimer in cells (*SI Appendix*, Fig. S1*B*).

A portion of the NS1-BP BTB dimer interface involves a domain swap in which the first β-strand (residues 1–12) of one subunit interacts with the fifth β-strand (residues 92–98) of the other subunit (Fig. 2*A*). We deleted residues 1–12 to destabilize the NS1-BP dimer (NS1-BPΔ1–12) (the difference in $\Delta G_{dissociation}$ predicted by PISA is 17.5 kcal/mol). Analytical ultracentrifugation analysis of NS1-BPΔ1–12 shows that the mutant equilibrates between monomer and dimer at 1 μM, 3 μM, and 9 μM (*SI Appendix*, Fig. S1*C*). NS1-BPΔ1–12 also forms higher-order oligomers at 3 μM and 9 μM (*SI Appendix*, Fig. S1*C*). The BTB dimer is indeed destabilized in the NS1-BPΔ1–12 mutant. We stably expressed either full-length NS1-BP or the dimer-destabilized NS1-BPΔ1–12 mutant in cells transfected with control siRNA or siRNA to knock down NS1-BP RNA and assessed influenza virus M1 to M2 mRNA splicing. RNA was purified from these cells, and M1/M2 mRNA levels were determined by qPCR. Destabilization of the NS1-BPΔ1–12 dimer prevented proper splicing of M1 to M2 mRNA (Fig. 2 *C* and *D*), indicating that a stable NS1-BP dimer is important for NS1-BP splicing activity. To further test the importance of dimerization, we replaced the BTB domain with the GCN4 coiled-coiled dimerization domain. The dimeric NS1-BP(GCN4 coiled-coil) mutant maintained its splicing activity, demonstrating that dimerization, whether through the BTB domain or through a generic coiled-coil, is required for NS1-BP splicing activity (Fig. 2 *C* and *D*). We also show that the BTB domain alone is not sufficient for the splicing activity of NS1-BP (Fig. 2 *C* and *D*), indicating that other NS1-BP domains promote splicing.

**BACK Domain of NS1-BP Recruits Splicing and mRNA Export Factors.** The BACK domain of NS1-BP connects the BTB and Kelch domains. BACK domains contain multiple tandem helical repeats

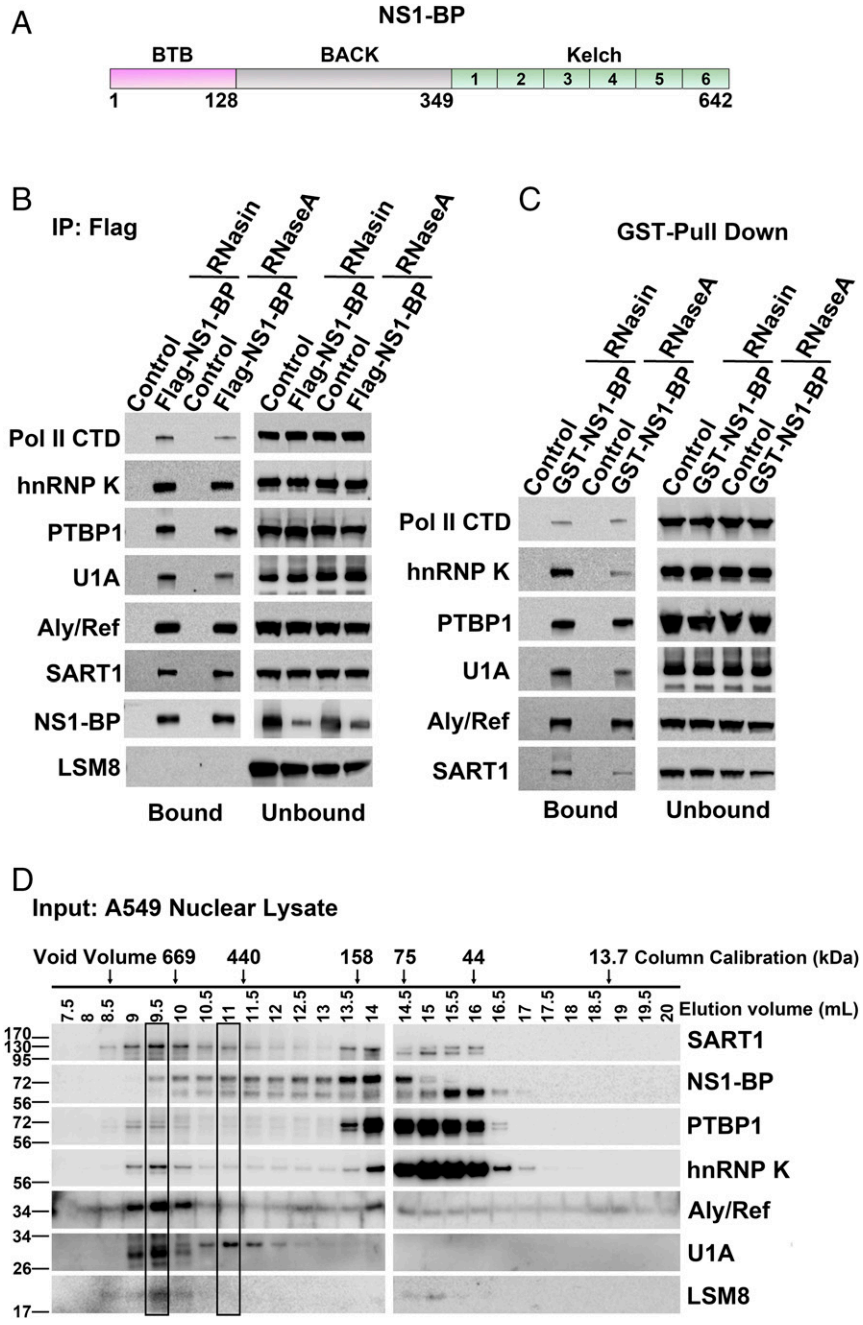


**Fig. 1.** NS1-BP interacts with splicing and mRNA nuclear export factors. (*A*) Schematic representation of the NS1-BP domains. (*B*) Cell extracts from A549 cells stably expressing the 3×Flag epitope alone or 3×Flag-NS1-BP were untreated or treated with RNasin or RNase A and subjected to immunoprecipitation with anti-Flag antibody followed by Western blot with specific antibodies to detect the depicted proteins. (*C*) Purified recombinant GST-NS1-BP or GST control incubated with extracts from A549 cells untreated or treated with RNasin or RNase A. In vitro binding assays were performed followed by Western blot to detect the depicted proteins in bound and unbound fractions. (*D*) Nuclear extracts from A549 cells were subjected to size-exclusion chromatography, and eluted fractions were analyzed by Western blot with specific antibodies to detect the depicted proteins.

that are reminiscent of HEAT repeats (KHLH3; PDB ID codes: 4AP2 and 2EQX). Secondary structure prediction suggests that the BACK domain of NS1-BP also contains multiple tandem α-helices. The sequences of these helices in NS1-BP align well with helices in the KLHL11 BACK [23% sequence identity; PDB ID code: 4AP2 (28)], suggesting that the NS1-BP BACK is also likely a series of five tandem helical repeats. Our inability to crystallize the NS1-BP BACK domain alone or with the BTB domain suggests that the BACK helical repeats may be flexible, as in many HEAT repeat proteins (13). We found that the BACK domain of NS1-BP binds splicing factors (hnRNP K, PTBP1, and U1A) and the mRNA export factor Aly/REF (Fig. 3 *A* and *B*). We have previously shown that the interaction of NS1-BP with hnRNP K is important in influenza virus RNA splicing (7, 9), but the NS1-BP domain that mediates this interaction had not been determined. In addition, the interaction of NS1-BP with PTBP1 and U1A had not been previously identified. These interactions were first detected in nuclear extracts as shown in *SI Appendix*, Table S1. These findings indicate binding of the NS1-BP BACK domain to the spliceosomal protein U1A and splicing factors PTBP1 and hnRNP K. PTBP1 has been previously shown to bind hnRNP K (29), further supporting our findings that both proteins interact with the same domain of NS1-BP. Moreover, the BACK domain of NS1-BP binds to the mRNA export factor Aly/REF, which associates with the spliceosome at late stages of splicing to link splicing to mRNA nuclear export (23). This is consistent with the size-exclusion chromatography results shown in Fig. 1*D* in which Aly/REF coeluted in a high molecular weight complex with spliceosome components and splicing regulators.

In vitro binding assays using purified recombinant Aly/REF and NS1-BP or U1A and NS1-BP show no direct binding between the proteins (Fig. 3*C*), indicating that interactions of NS1-BP with Aly/REF and U1A are indirect. However, purified PTBP1 and hnRNP K bound directly to the BACK domain of NS1-BP, as does the

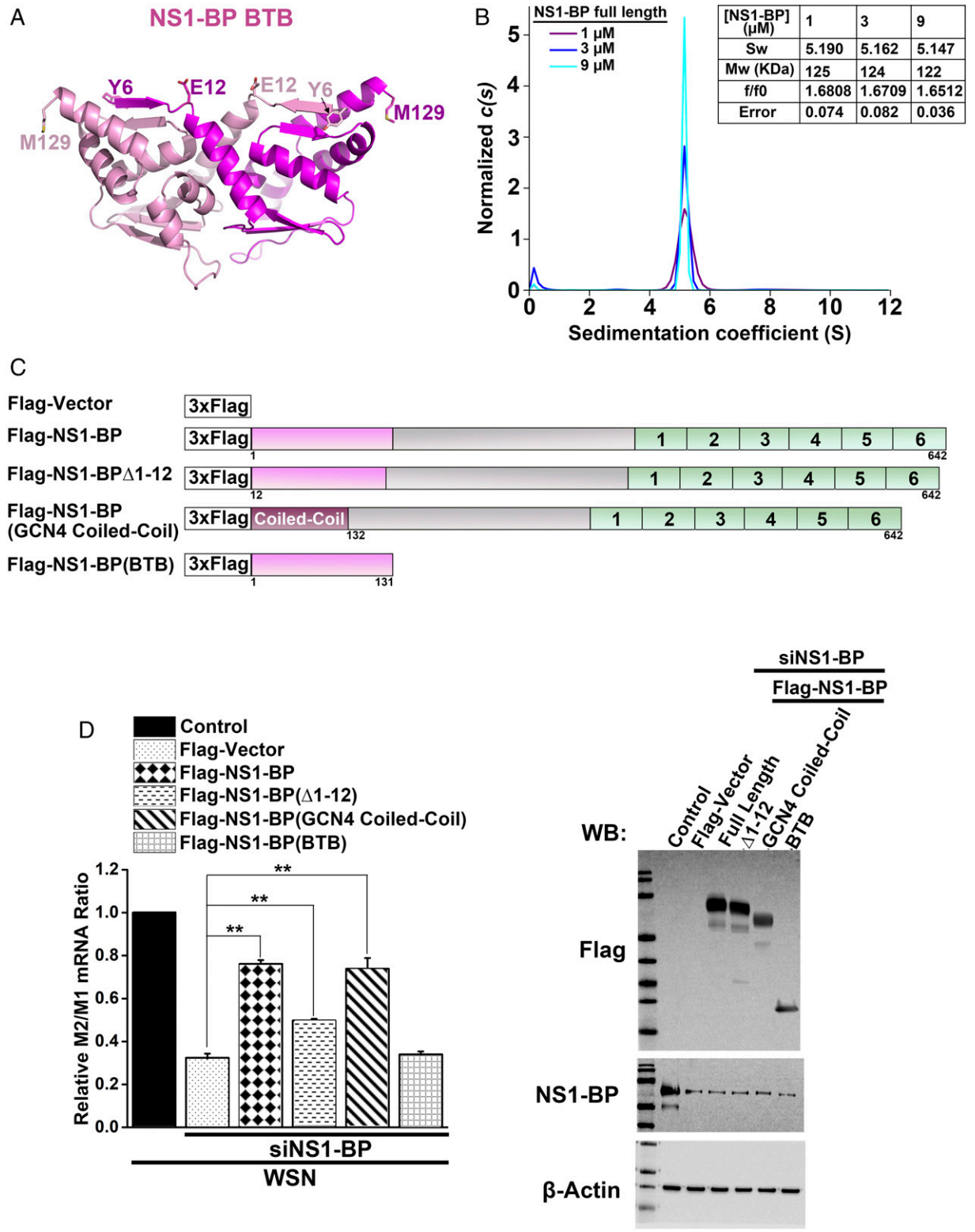


**Fig. 2.** Homodimerization of the BTB domain of NS1-BP is critical for NS1-BP splicing activity. (*A*) The crystal structure of the BTB domain of NS1-BP (residues 6–129) with one subunit of the BTB dimer shown in magenta and the other in pink. Residues in the N-terminal–most β-strands of both subunits are labeled, as that β-strand is deleted to generate mutant NS1-BPΔ1–12. (*B*) The sedimentation properties of 1 μM, 3 μM, and 9 μM purified NS1-BP were compared by sedimentation velocity analysis and the size distributions, c(S) (sedimentation coefficient distribution normalized for absorption differences), of the three samples are plotted. The sedimentation coefficients (Sw), molecular weights (Mw) (estimated from the best-fit frictional ratio, f/f0), and errors are also shown in the *Inset*. (*C*) Schematic representation of proteins studied in this figure. (*D*, *Left*) RNA was purified from A549 cells stably expressing the depicted proteins and depleted of endogenous NS1-BP by siRNA targeting the 3′ UTR, or control siRNA, followed by infection with influenza virus (WSN) at a multiplicity of infection (MOI) of 2 for 7 h. qPCR was performed to determine the ratio of influenza virus M2/M1 mRNAs. $n = 3$; $^{**}P < 0.01$. (*Right*) Gels depict the expression levels of each depicted protein, endogenous NS1-BP, and β-actin (control), as determined by Western blot.

influenza virus NS1 protein, which first led to the discovery of NS1-BP (Fig. 3 *D*–*F*) (15). NS1 binding to the BACK domain does not compete with hnRNP K or PTBP1 (*SI Appendix*, Fig. S2). PTBP1 was previously reported to bind hnRNP K (29). Binding assays with purified proteins show that NS1 binds NS1-BP but not hnRNP K and that NS1-BP binds to both hnRNP K and NS1 (Fig. 3*G*), indicating that NS1-BP bridges the interactions between NS1 and hnRNP K. In summary, the BACK domain of NS1-BP binds directly to PTBP1, hnRNP K, and NS1 but interacts only indirectly with U1A and Aly/REF. These findings support a role for NS1-BP in splicing and mRNA nuclear export. The latter is addressed further below.

**The Kelch Domain of NS1-BP Binds Splicing Factors and Is Required for Splicing.** We solved the crystal structure of the NS1-BP Kelch domain to 2.6-Å resolution. The domain is composed of six Kelch β-propeller repeats or blades (Fig. 4*A*). Each Kelch repeat is a four-stranded antiparallel β-sheet, and the six repeats are positioned radially around a central axis. Loops that connect the β-strands in the domain protrude from the top and bottom of the disk-shaped domain. Long loops that connect the second and third β-strands of each Kelch repeat/blade (R1Loop, R2Loop, R3Loop, R4Loop, R5Loop, and R6Loop) protrude to the top of the domain (Fig. 4*B*) and were found to be ligand-binding sites in several Kelch domains (30–32). Kelch domains are known to be protein–protein interaction modules, and in NS1-BP the Kelch domain binds SART1 and the Pol II CTD, as shown in cells expressing full-length NS1-BP or domain-deletion mutants that were subjected to immunoprecipitation followed by Western blot analysis (Fig. 4*C*). In an attempt to map ligand-binding sites in the Kelch domain, we truncated individual R1–R6 loops and assessed the ability of the truncated-loop mutant NS1-BPs to bind SART1 and the Pol II CTD. NS1-BP mutants with a truncated R2Loop or a truncated R3Loop (circular dichroism spectra show they are folded) (*SI Appendix*, Fig. S3) showed decreased SART1 and Pol II CTD binding (Fig. 4*D*), suggesting that these loops may be part of the binding sites.

SART1 (or Snu66) is a member of the U4/U6-U5 trisnRNP and is involved in spliceosome activation (22), whereas the Pol II CTD interacts with the virus polymerase (33, 34), which has a role in the choice of alternative 5′ splice sites in the influenza virus M1 mRNA (35). The interactions of the Kelch domain with a spliceosome factor and with a splicing regulator suggest this domain has an important role in NS1-BP function in splicing. Indeed, we show that the Kelch domain of NS1-BP is required for splicing of M1 to M2 mRNA in influenza virus-infected cells expressing full-length NS1-BP or specific deletion mutants of NS1-BP domains (Fig. 4*E*). Replacement of the NS1-BP Kelch domain by the hKLHL2 Kelch domain did not rescue NS1-BP splicing activity, indicating that the Kelch domain of NS1-BP has features important for its splicing function (Fig. 4*E*). Additionally, a smear is present above the BTB-BACK protein, suggesting that it may be posttranslationally modified, a potential regulatory process that should be investigated in the future.

**NS1-BP's Role in mRNA Nuclear Export.** As shown above, NS1-BP binds the mRNA nuclear export factor Aly/REF through its BACK domain (Figs. 1 and 3), suggesting a role in viral M mRNA nuclear export. To further define the function of NS1-BP in viral mRNA nuclear export, A549 cells stably expressing full-length NS1-BP or mutants of NS1-BP were infected for 4 h or 8 h and were subjected to single-molecule RNA (smRNA)-FISH to determine the intracellular localization of M mRNA (Fig. 5 and *SI Appendix*, Fig. S4). At 4 h postinfection, most of the M mRNA is still nuclear (Fig. 5*A*). However, expression of full-length NS1-BP or NS1-BP BTB-BACK domains promoted nuclear export of M mRNA to the cytoplasm at 4 h postinfection (Fig. 5*A*), although the full-length protein was slightly more efficient in inducing export. On the other hand, expression of the BTB and the first half of the BACK domain (BTB-BACK1, amino acids 1–234), which lacks the binding site for the mRNA export factor Aly/REF, did not promote M mRNA nuclear export at 4 h postinfection (Fig. 5*A*). A similar pattern was observed at 8 h postinfection. At this time, most of the M mRNA is already cytoplasmic, and overexpression of full-length NS1-BP or its BTB-BACK further enhanced its cytoplasmic localization (Fig. 5*B*). On the other hand, expression of BTB-BACK1 blocked M mRNA in the nucleus (Fig. 5*B*). We have also performed these experiments with the viral HA mRNA (*SI Appendix*, Fig. S5) and NS mRNA (*SI Appendix*, Fig. S6). As opposed to the viral M mRNA, wild-type or mutants of NS1-BP had no effect on the intracellular distribution of the HA and NS mRNAs. In addition, we observed no changes in NS1 mRNA or protein levels or in the NS2/NS1 mRNA ratios, as NS mRNA also undergoes alternative splicing (*SI Appendix*, Fig. S7). We have also tested M vRNP and show that NS1-BP enhances its nuclear export at 8 h postinfection and the NS1-BP BTB-BACK1 is sufficient to promote this effect (*SI Appendix*, Fig. S8). These results revealed that NS1-BP has the activity of an RNA nuclear export factor, as its expression promotes trafficking of viral M mRNA and vRNP out of the nucleus, and that the BACK domain binds an mRNA export factor involved in this process.

**NS1-BP Alters Cellular mRNA Levels.** Since viral–host interactions traditionally uncover new cellular functions, the cellular NS1-BP protein functions likely impact cellular mRNAs. To determine if this is indeed the case, RNA purified from control or NS1-BP–knockdown cells was subjected to RNA-sequencing (RNA-seq) analysis. From 56,634 RNAs sequenced, 667 mRNAs were altered by NS1-BP depletion (428 were down-regulated, and 239 were up-regulated), considering a cutoff of 1.5-fold (*SI Appendix*, Table S3). RNA-seq was also performed in cells stably expressing NS1-BP with siRNAs against NS1-BP to identify high-confidence hits (Dataset S1). Overlapping hits were detected between this condition and the condition described in *SI Appendix*, Table S3, in which endogenous NS1-BP was knocked down. While there were overlapping mRNAs, we have detected mRNAs that were specific for each condition. This is likely because stable expression of NS1-BP, even in the presence of NS1-BP knockdown, yields levels of this protein slightly higher than endogenous levels, as it is difficult to obtain exact endogenous conditions. Since NS1-BP is involved in gene expression, the differences observed are expected. Nevertheless, gene set enrichment analysis (GSEA) of both conditions revealed the matrisome and the reactome immune system (Fig. 6 *A* and *B* and Dataset S1). Selected top hits were then confirmed by qPCR to determine total levels (Fig. 6*C*) or the intracellular distribution between the nucleus and cytoplasm (Fig. 6*D*). We found that NS1-BP altered the levels and/or nuclear export of a subset of cellular mRNAs, indicating that NS1-BP functions on the expression and localization not only of a viral mRNA but also of key cellular mRNAs, such as CENPK, SKP2, RAB9A, NOTCH3, SERF1A, PIK3R2, and others. Together, these findings underscore the impact of NS1-BP on the expression of factors involved in cell growth and in the influenza virus life cycle.

## Discussion

This study uncovered interactions of NS1-BP with key constituents of the splicing and mRNA nuclear export machineries, which support its function in splicing and nuclear export. All domains of NS1-BP are essential for its function in splicing, while only the BACK domain is required for the mRNA export activity of NS1-BP. With regards to splicing, we show here that the BTB domain mediates the required dimerization of NS1-BP, while the BACK and Kelch domains function as protein–protein interaction modules to recruit proteins involved in splicing. Specifically, the Kelch domain recruits SART1 (22) and the Pol II CTD (36), whereas the BACK domain recruits hnRNP K, U1A, PTBP1, and the viral protein NS1 (7–9). The BACK domain also recruits Aly/Ref to mediate mRNA export.

The BACK domain of NS1-BP interacts directly with hnRNP K and PTBP1. However, the interactions between the BACK

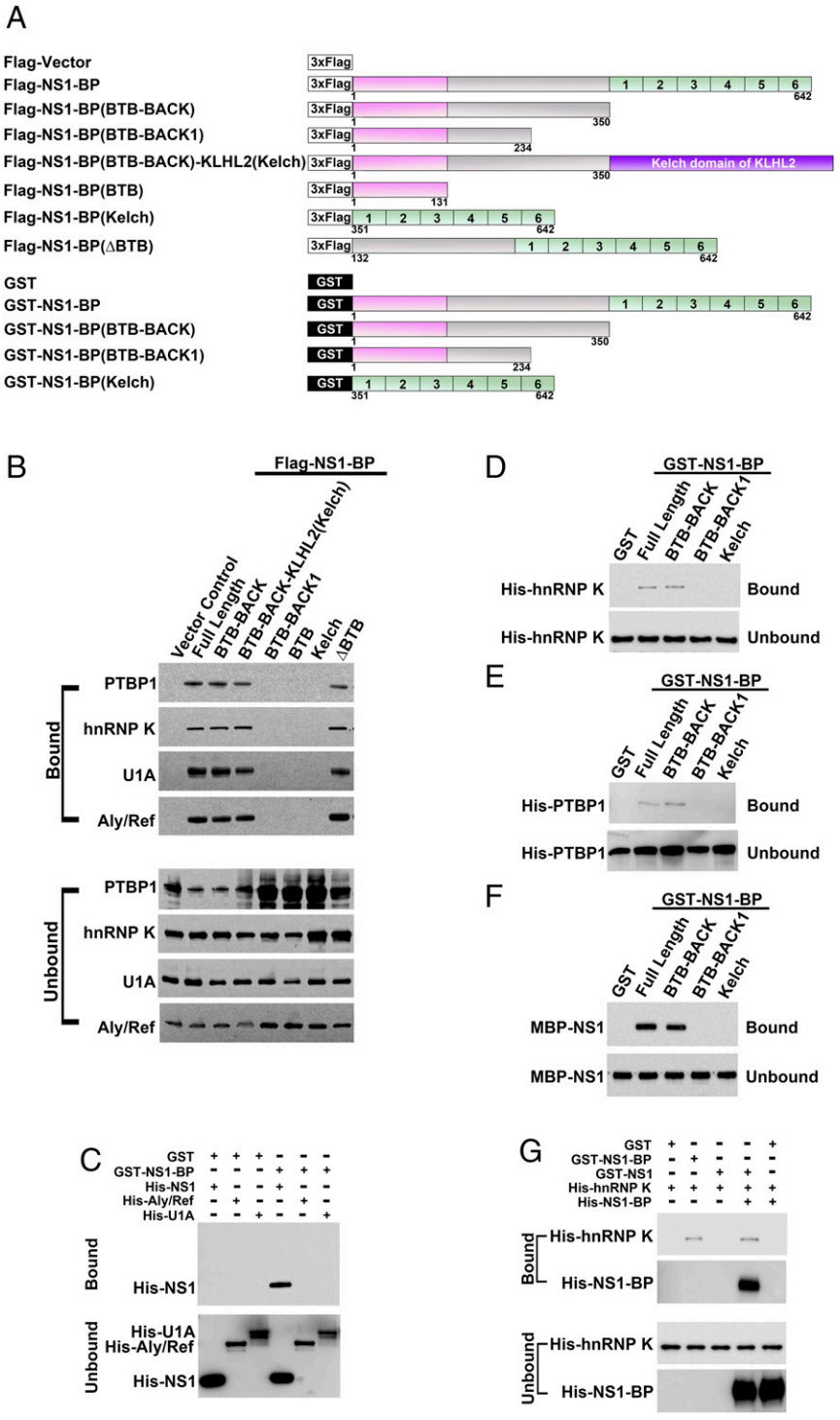


**Fig. 3.** The BACK domain of NS1-BP interacts with splicing and mRNA export factors. (*A*) Schematic representation of proteins studied in this figure. (*B*) Cell extracts from A549 cells stably expressing the depicted NS1-BP wild-type and mutant proteins were subjected to immunoprecipitation with anti-Flag antibody followed by Western blots with specific antibodies against the depicted proteins. Bound and unbound fractions are shown. Expression and immunoprecipitation efficiency for each Flag-tagged protein are shown in *SI Appendix*, Fig. S9*C*. (*C*–*G*) In vitro binding assays were performed with the depicted combinations of purified recombinant proteins. Bound and unbound fractions were subjected to Western blot to detect the depicted proteins.

domain and U1A and Aly/Ref are indirect. PTBP1 is known to interact with hnRNP K (29), which binds directly to the viral M mRNA, as we previously reported (9). Since U1A binds U1 snRNA, which interacts with the 5′ splice site of pre-mRNAs to mediate the first steps of splicing (22), and PTBP1 represses the early stages of splicing (37), the NS1-BP BACK domain and hnRNP K likely interact with the PTBP1 complex to mediate or regulate the early stages of splicing. Furthermore, the Kelch domain of NS1-BP binds the Pol II CTD that interacts with the virus polymerase (33, 34). The viral polymerase, in turn, mediates the choice of alternative 5′ splice sites in the influenza virus M1 mRNA by blocking the 5′ splice site that generates the noncoding $mRNA_3$ and causing the switch to the M2 mRNA 5′ splice site (35). Additionally, NS1-BP probably continues to participate in the splicing reaction, as its Kelch domain interacts with SART1, a constituent of the U4/U6-U5 trisnRNP that functions in spliceosome assembly (22). Thus, it is possible that the Kelch domain interaction with the Pol II CTD occurs at the early stages of splicing, while its binding to SART1 takes place at the later stage of spliceosome activation.

The mRNA export factor Aly/REF interacts indirectly with the BACK domain of NS1-BP in an RNA-independent manner, whereas hnRNP K bound directly to this domain. Both hnRNP

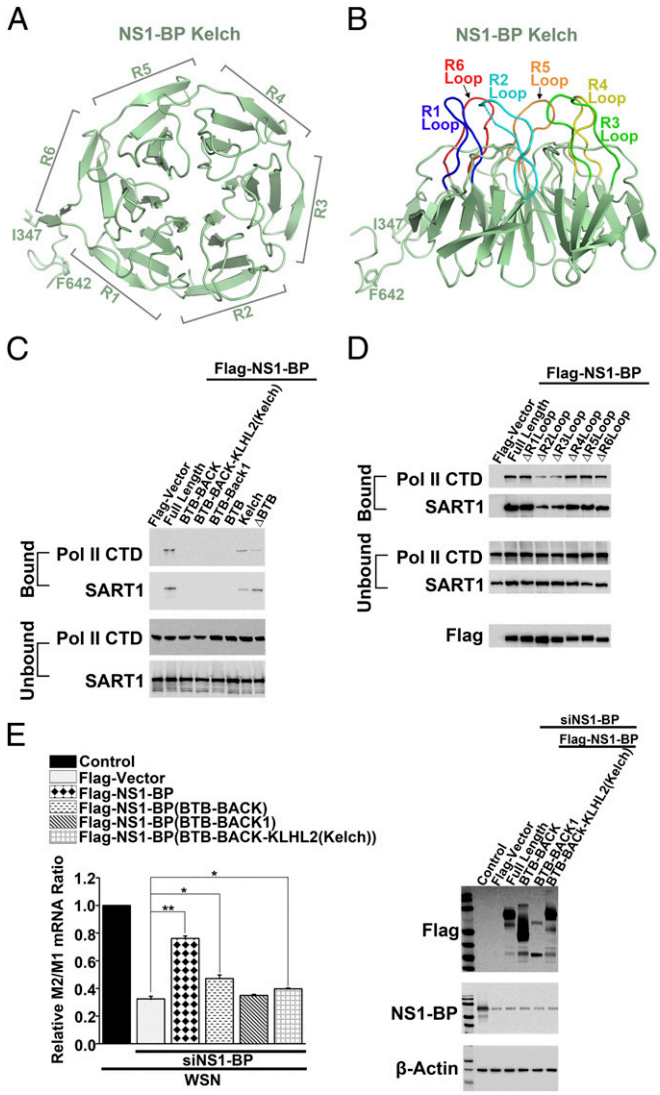


**Fig. 4.** The Kelch domain of NS1-BP binds spliceosome factors and is required for splicing. (*A*) Crystal structure of the Kelch domain of NS1-BP (residues 347–642; six tandem histidine residues are at the C terminus of Phe642); the six blades or repeats of the β-propeller domain are labeled R1–R6. (*B*) A view of the Kelch domain rotated 90° about the horizontal axis from the orientation in *A*. Each Kelch repeat/blade contains a long R1Loop (blue), R2Loop (cyan), R3Loop (green), R4Loop (yellow), R5Loop (orange), and R6Loop (red) that connects their central β-strands. (*C*) A549 cells stably expressing full-length 3×Flag-NS1-BP or the various depicted mutants of NS1-BP were immunoprecipitated with anti-Flag antibody followed by Western blot to detect SART1 and Pol II CTD. Expression and immunoprecipitation efficiency for each Flag-tagged protein are shown in *SI Appendix*, Fig. S9*C*. (*D*) As in *C*, except that additional cells expressing full-length NS1-BP or NS1-BP with truncated individual loops were tested, as shown in *B*. (*E*, *Left*) RNA was purified from A549 cells stably expressing the depicted proteins and depleted of endogenous NS1-BP by siRNA targeting the 3′ UTR or control siRNA, followed by infection with influenza virus (WSN) at an MOI of 2 for 7 h. qPCR was performed to determine the ratio of influenza virus M2/M1 mRNAs. $n = 3$; $^{**}P < 0.01$ and $^{*}P < 0.05$. (*Right*) Gels depict the expression levels of each depicted protein, endogenous NS1-BP, and β-actin (control), as determined by Western blot.

K and Aly/REF are important for nuclear trafficking of the viral M mRNA (7), consistent with the role of the NS1-BP BACK domain in nuclear export of the viral M mRNA shown here. Additionally, the BACK domain interacts with the influenza virus NS1 protein, which promotes viral M mRNA splicing and export (7, 38). Thus, these interactions of the NS1-BP BACK domain with Aly/REF, hnRNP K, and NS1 likely work together to mediate M mRNA nuclear export, as shown here and supported by our previous results (7). The role of NS1-BP in mediating both splicing and nuclear export is consistent with the identification of other proteins that are involved in more than one step of gene expression, such as the TREX complex and SR proteins. The TREX complex of proteins, which includes Aly/REF, couples transcription to mRNA processing and nuclear export (39). Similarly, SR proteins can function throughout the gene-expression pathway from transcription, processing, and nuclear export to translation (40).

NS1-BP activities impact a subset of influenza virus mRNAs. While the splicing of the M mRNA is mediated by NS1-BP, the NS mRNA splicing is not affected by NS1-BP (9). In addition, nuclear export of viral HA and NS mRNAs is not altered by NS1-BP. However, nuclear export of M vRNP was enhanced by NS1-BP but required a different region of the BTB-BACK domain than the M mRNA. This is an interesting observation for future studies. Regarding cellular mRNAs, we show that depletion of NS1-BP affected RNA levels and intracellular distribution of only a subset of mRNAs. These results suggest that NS1-BP has a role in the expression and/or nuclear export of a subset of viral and cellular mRNAs. Interestingly, this subset enriched for mRNAs that encode immune factors and proteins involved in tumorigenesis. As mentioned above, NS1-BP and hnRNP K have roles in cancer metastasis (19, 20). This is consistent with our findings that NS1-BP regulates subsets of mRNAs encoding constituents of the p53 pathway, the matrisome, and platelet activation signaling and aggregation, which are directly involved in various stages of tumorigenesis (41, 42). The role of NS1-BP in immunity is probably a result, at least in part, of the viral–host interactions shown here which impact virus replication (7, 9, 15). In sum, NS1-BP functions target a subset of viral and cellular mRNAs that encode critical mediators and regulators of viral infection, cell growth, and immunity.

## Materials and Methods

**Reagents and Plasmids.** See *SI Appendix* for detailed information.

**Crystallization and Structure Determination.** Crystals were grown in 96-well plates by using sitting-drop vapor diffusion at 20 °C (0.4 μL protein + 0.4 μL reservoir solution). The reservoir solution for the BTB domain was 0.2 M ammonium sulfate, 0.1 M Tris (pH 8.5), and 25% (wt/vol) polyethylene glycol 3350 and for the Kelch domain was 0.1 M Tris (pH 8.5) and 3.0 M NaCl. Crystals were cryoprotected by the addition of ∼20% (vol/vol) ethylene glycol and were flash-cooled by immersion in liquid nitrogen. The datasets were collected at the Advance Photon Source (APS)19 ID beamline in the Structural Biology Center at Argonne National Laboratory. The BTB domain crystal was diffracted to 2.8-Å resolution, and the Kelch domain crystal was diffracted to 2.6-Å resolution. Data were indexed, integrated, and scaled using HKL3000 (43). The structures were solved by molecular replacement using PHASER in the Phenix software package (44, 45). The structure of the BTB-BACK domains of human KLHL11 (PDB ID code: 3I3N) and the Kelch domain of human KLHL2 (PDB ID code: 2XN4) were used as the search models for the BTB domain and Kelch domain of NS1-BP, respectively. Subsequent iterative model building and refinement were performed with Phenix and Coot (44, 46). Illustrations were prepared with PyMOL (Schrodinger: https://www.schrodinger.com/pymol).

**GST Pull-Down Assays.** GST or GST fused with NS1-BP was incubated with A549 total cell lysate in lysis buffer [50 mM Tris, 150 mM NaCl, 1 mM EDTA, 1 mM DTT, 1% IGEPAL CA-630 (Sigma Aldrich), 0.1 mM $Na_3VO_4$, 1 mM NaF, 1 mM PMSF, 1× cOmplete protease inhibitor mixture (Sigma Aldrich), and 10% glycerol, pH 7.5] at 4 °C for 4 h. GST or GST fused with NS1-BP or with its mutants NS1-BPΔKelch, NS1-BP-BTB-BACK1 (amino acids 1–234), or NS1-BP-Kelch (amino acids 351–642) was bound to glutathione beads and incubated with His-hnRNP K, His-PTBP1, His-ALYREF, His-U1A, His-NS1, or MBP-NS1 in the pull-down buffer (20 mM Tris, 150 mM NaCl, 1 mM DTT, 1 mM EDTA, pH 7.5) at 4 °C for 2 h. GST or GST fused with NS1 was incubated with His-hnRNP K in the absence or presence of His-NS1-BP in the pull-down buffer at 4 °C for 2 h. One micromolar of each protein was loaded into the pull-down assay. Beads were pelleted by centrifuging at 2,300 × *g* for 5 min and were washed five

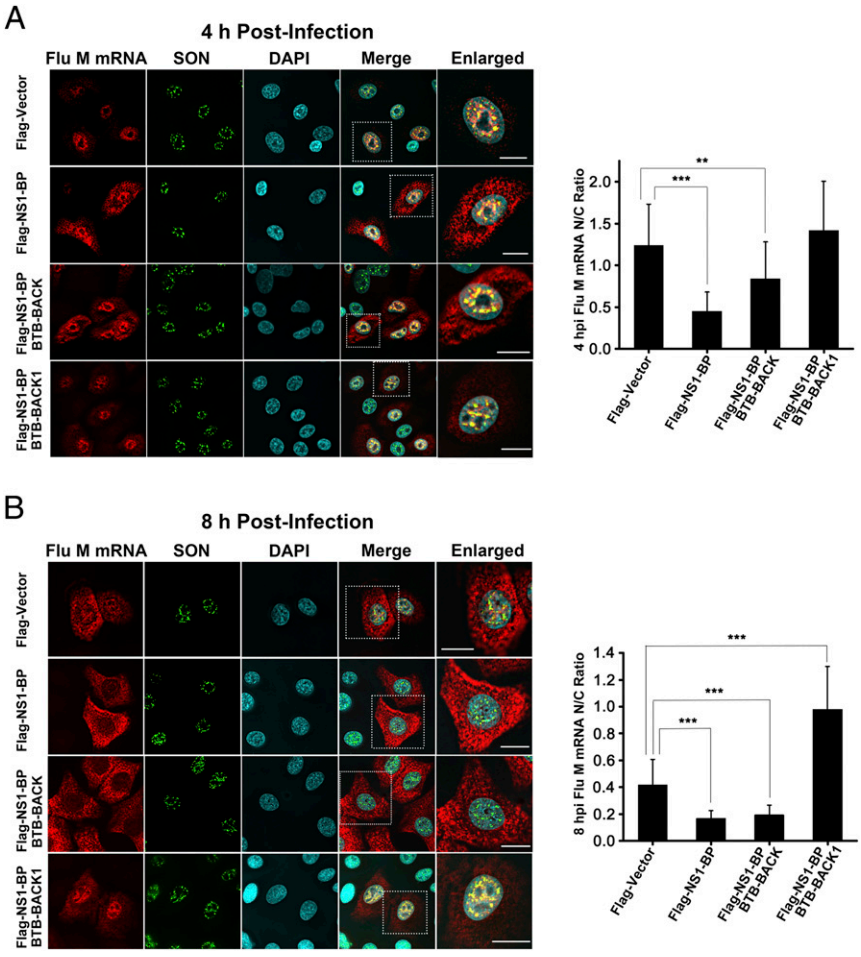


**Fig. 5.** The BACK domain of NS1-BP mediates viral M mRNA nuclear export. A549 cells stably expressing the depicted proteins were infected with influenza virus (WSN) at an MOI 2 for 4 h (*A*) or 8 h (*B*) and were then subjected to smRNA-FISH to detect the intracellular distribution of viral M mRNA. Immunofluorescence was performed simultaneously to detect nuclear speckles, which are labeled with SON antibody. DNA was stained with Hoechst. Histograms depict the M mRNA nuclear-to-cytoplasmic (N/C) ratios determined by quantification of fluorescence intensity in both compartments. Values shown are means ± SD measured in 50 cells. $***P < 0.001$ and $**P < 0.01$. (Scale bar: 10 μM.) Intracellular localization of Flag-NS1-BP wild-type and mutant proteins is presented in *SI Appendix*, Fig. S4 and shows distribution in the nucleus and cytoplasm similar to that of endogenous NS1-BP.

times with 1 mL of pull-down buffer. Proteins remaining on the resin were extracted by sample buffer, resolved in SDS/PAGE, and then detected by Western blot.

**Virus.** Influenza A virus A/WSN/1933 (WSN) was propagated in MDCK cells and was titered as previously described (9). All virus work was performed in strict accordance with CDC guidelines for biosafety level 2.

**Stable Cell Lines.** Full-length NS1-BP and its mutants NS1-BP BTB (amino acids 1–131), NS1-BPΔ1–12, NS1-BP-BTB/GCN4-coiled-coil, NS1-BP BTB-BACK (amino acids 1–350), NS1-BP BTB-BACK1 (amino acids 1–234), NS1-BP-Kelch/hKLHL2-Kelch, NS1-BP Kelch (amino acids 351–642), and NS1-BP ΔBTB (amino acids 132–642) were cloned into pCDH-CMV-MCS-EF1-puro with the 3×Flag tag at the N terminus. One thousand nanograms of each plasmid, together with 250 ng pVSV-G plasmid and 750 ng pCMVΔR9 plasmid were reverse-transfected into 293T cells using the TransIT-X2 Dynamic Delivery System (Mirus Bio) to generate lentiviruses carrying the inserted gene. Vector expressing the 3×Flag tag was used as control. At 60 h posttransfection, all supernatants containing viruses were collected and were used to infect A549 cells in a 12-well plate to stably express the inserted genes. At 24 h postinfection, cells were transferred to a 15-cm dish and were cultured in the presence of 1 μg/mL puromycin. Puromycin-resistant single clones were collected and transferred to six-well plates in the presence of 1 μg/mL puromycin. Expression of inserted genes was tested by Western blot using mouse anti-Flag antibody.

**Cell Fractionation.** Cells were harvested by trypsinization and collected in 15-mL conical tubes on ice, washed three times with cold PBS, and transferred to microfuge tubes. Cell fractionation was performed using the NE-PER Nuclear and Cytoplasmic Extraction Reagents (Thermo Fisher Scientific) according to the manufacturer's instructions. Controls for fractionation are shown in *SI Appendix*, Fig. S9*D*.

**Immunoprecipitation and Mass Spectrometry.** A549 cells stably expressing 3×Flag vector control, 3×Flag-NS1-BP, and 3×Flag-NS1-BP BTB-BACK were cultured in 10-cm plates and fractionated as described above. The nuclear fraction was lysed in 50 mM Tris (pH 7.5), 150 mM NaCl, 1% IGEPAL CA-630, 0.1 mM $Na_3VO_4$, 1 mM NaF, 1 mM DTT, 1 mM EDTA, 1 mM PMSF, 1× cOmplete protease inhibitor mixture, and 10% glycerol, for 30 min on ice, homogenizing with vortex. Cell lysates were centrifuged at 13,000 × *g* for 10 min to remove cellular debris. The supernatant was applied to Anti-FLAG M2 magnetic beads (Sigma Aldrich) in the presence of 1 μg/mL RNase A and 1 μg/mL DNase for binding overnight at 4 °C. Beads were washed five times with lysis buffer at 4 °C. Then proteins were eluted using 3×Flag peptide. The eluted fractions were mixed with sample buffer and subjected to 10% SDS/PAGE. Gel was then stained with Colloidal Blue (Thermo Fisher Scientific). Each lane was excised into three fragments containing proteins above 17 kDa. Gel slices were subjected to in-gel trypsin digestion followed by LC/MS/MS analysis. Data were analyzed against the National Center for Biotechnology Information nonredundant (NCBI-nr) protein database with Mascot software (Matrix Science). To confirm the binding of identified proteins to NS1-BP, cell lysates from A549 cells stably expressing 3×Flag vector (control) or 3×Flag-NS1-BP were loaded to Anti-FLAGM2 magnetic beads in the presence of 1 μg/mL RNase A and 1 μg/mL DNase at 4 °C for 6 h. Beads were washed five times with lysis buffer. The bound proteins were eluted with 3×Flag peptide. Samples were mixed with 5× sample buffer, boiled, and subjected to Western blot.

**Size-Exclusion Chromatography.** A549 cells were grown to 90–100% confluency and were fractioned as above. The nuclear fraction was lysed in 50 mM Tris (pH 7.5), 150 mM NaCl, 1% IGEPAL CA-630, 0.1 mM $Na_3VO_4$, 1 mM NaF, 1 mM DTT, 1 mM EDTA, 1 mM PMSF, 1× cOmplete protease inhibitor mixture, and 15% glycerol and then was loaded onto a Superdex 200 Increase 10/300 GL column (GE Healthcare) in a buffer containing 20 mM Tris, 150 mM NaCl, 1 mM EDTA, 1 mM DTT, 1× cOmplete protease inhibitor mixture, and 5% glycerol. Half-milliliter fractions were collected from the elution volume of

A

| Enriched Pathways of mRNAs Downregulated upon NS1-BP Knock Down | | | | | |
|---|---|---|---|---|---|
| GSEA Pathways | # Genes in Pathway (S) | # Genes Overlap with Hits (H) | H/S Ratio | p-value | FDR q-value |
| REACTOME_PLATELET_ACTIVATION_SIGNALING_AND_AGGREGATION | 208 | 17 | 0.0817 | 2.74E-12 | 3.64E-09 |
| REACTOME_HEMOSTASIS | 466 | 20 | 0.0429 | 3.45E-09 | 2.14E-06 |
| REACTOME_METABOLISM_OF_LIPIDS_AND_LIPOPROTEINS | 478 | 20 | 0.0418 | 5.30E-09 | 2.14E-06 |
| PID_VEGFR1_2_PATHWAY | 69 | 9 | 0.1304 | 6.44E-09 | 2.14E-06 |
| REACTOME_IMMUNE_SYSTEM | 933 | 27 | 0.0289 | 3.01E-08 | 8.01E-06 |

B

| Enriched Pathways of mRNAs Upregulated upon NS1-BP Knock Down | | | | | |
|---|---|---|---|---|---|
| GSEA Pathways | # Genes in Pathway (S) | # Genes Overlap with Hits (H) | H/S Ratio | p-value | FDR q-value |
| NABA_MATRISOME | 1028 | 19 | 0.0185 | 2.54E-07 | 3.38E-04 |
| PID_P53_DOWNSTREAM_PATHWAY | 137 | 7 | 0.0511 | 3.19E-06 | 2.12E-03 |
| KEGG_PATHWAYS_IN_CANCER | 328 | 9 | 0.0274 | 2.02E-05 | 7.59E-03 |
| PID_AVB3_INTEGRIN_PATHWAY | 75 | 5 | 0.0667 | 2.36E-05 | 7.59E-03 |
| REACTOME_SIGNALING_BY_SCF_KIT | 78 | 5 | 0.0641 | 2.86E-05 | 7.59E-03 |

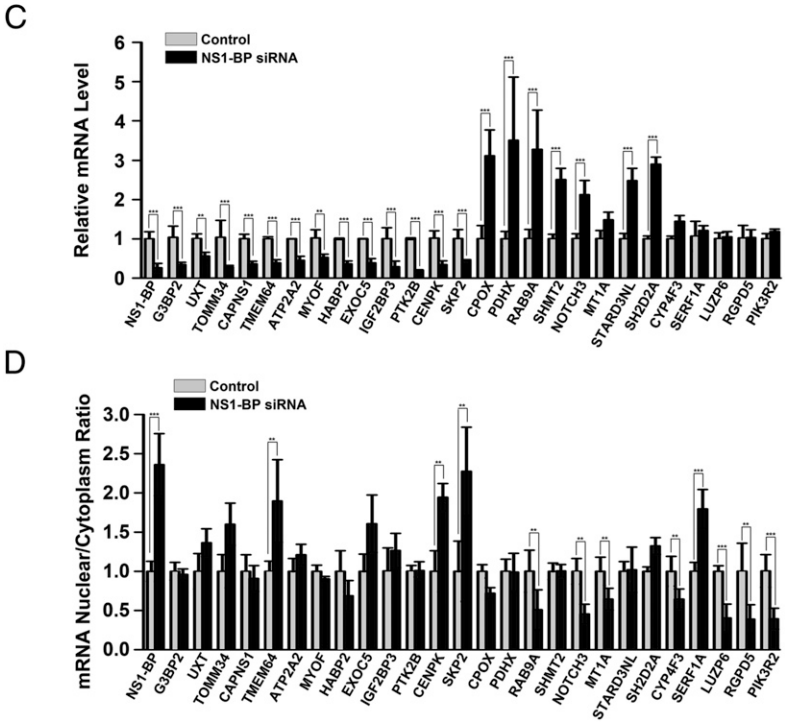


**Fig. 6.** NS1-BP alters the levels of a subset of mRNAs that encode proteins involved in cancer metastasis and immunity. (*A* and *B*) RNA from A549 cells transfected with control siRNAs or with siRNAs to knock down NS1-BP was subjected to RNA-seq followed by GSEA. The top five pathways are shown with the percentage overlap between total genes (S) in the pathway versus overlapping genes (H). *P* values for statistical significance and *q* values for FDR are shown. (*C*) Selected top mRNA hits from the RNA-seq analysis in *A* were validated by qPCR. $n = 3$; $^{***}P < 0.001$. (*D*) RNA was purified from nuclear and cytoplasmic fractions from the cells in *A*, and the selected mRNA hits from *C* were quantified by qPCR followed by determination of nuclear-to-cytoplasmic ratios. $n = 3$; $^{***}P < 0.001$ and $^{**}P < 0.01$.

7.5–20 mL, and 450 μL of each fraction was precipitated with 2% trichloroacetic acid with eight volumes of cold acetone, as previously described (9). Pellets were resuspended in sample buffer and subjected to Western blot.

**Analytical Ultracentrifugation.** The sedimentation properties of NS1-BP and NS1-BPΔ1–12 were compared in sedimentation velocity experiments performed in a Beckman-Coulter Optima XL-I Analytical Ultracentrifuge. NS1-BP and NS1-BPΔ1–12 were analyzed at three different concentrations (1 μM, 3 μM, and 9 μM) in analytical ultracentrifugation (AUC) buffer containing 20 mM Tris (pH 8.0), 150 mM NaCl, 1 mM EDTA, and 1 mM TCEP. Protein samples (400 μL) and AUC buffer (400 μL) were loaded into a double-sector centerpiece and centrifuged in an eight-cell An-50Ti rotor to 50,000 rpm at 20 °C. The double sectors were monitored for absorbance at 280 nm ($A_{280}$). A total of 140 scans was collected, and the first 40 scans were analyzed. Buffer density, viscosity of the buffer, and partial specific volume of the protein were estimated using SEDNTERP (rasmb.org/sednterp/). Sedimentation coefficient [c(S)] distribution values (normalized for absorption differences) were calculated by least-squares boundary modeling of sedimentation velocity data using the SEDFIT program (47). Sedimentation coefficients (Sw) [weight-average obtained from the integration of c(S) distribution], molecular weights (Mw) (estimated from the best-fit frictional ratio), and frictional ratios (f/f0) were obtained by refining the fit data in SEDFIT (48). Sedimentation coefficient distributions were converted to molar mass distributions based on the f/f0 ratio in SEDFIT (48) wherever possible. For error reporting, F-statistics and Monte-Carlo were used for integrated weight-average s values. Data were plotted using GUSSI (48).

**RNAi and Transfection.** A549 cells stably expressing 3×Flag vector control or 3×Flag-NS1-BP or NS1-BP mutants [3×Flag-NS1-BPΔ1–12, 3×Flag-NS1-BP BTB/coiled-coil, 3×Flag-NS1-BP BTB, 3×Flag-NS1-BP BTB-BACK, 3×Flag-NS1-BP BTB-BACK1, and 3×Flag-NS1-BP (Kelch/hKLHL2-Kelch)] were reverse transfected with 50 nM nontargeting siRNA or 50 nM siRNA oligos, which target the 3′ UTR of IVNS1ABP, using RNAiMAX (Thermo Fisher Scientific) for 48 h. According to the manufacturer's instructions, 3 μL of RNAiMax was used for 50 pmol siRNA. Cells were seeded into 12-well plates at a density of $3 \times 10^5$ per well. Knockdown efficiency was determined by Western blot.

**RNA Purification and qPCR.** Total RNA from A549 cells stably expressing 3×Flag vector, 3×Flag NS1-BP, and NS1-BP mutants treated with siRNA targeting the NS1-BP 3′ UTR were isolated using the RNeasy Plus Mini Kit (Qiagen). One microgram of total RNA was used to generate cDNA by reverse transcription using SuperScript II Reverse Transcriptase (Thermo Fisher Scientific). cDNA was diluted at a ratio of 1:5. cDNA samples were mixed with specific primers and Roche 480 SYBR Green I Master real-time PCR reagents and were subjected to qPCR using the Roche

LightCycler 480 system. The program used for qPCR was previously reported (49). Primer sequences used for β-actin, M1, and M2 have been previously reported (9).

**RNA-Seq.** A549 cells were reverse transfected with 50 nM nontargeting siRNA or 50 nM siRNA oligos (SMARTpool) to target NS1-BP using RNAiMAX for 48 h. Total RNA was isolated by the RNeasy Plus Mini Kit and was subjected to RNA-seq. The RNA-seq data were tested for quality using FastQC (50). The sequence data were aligned to the human genome using TopHat (cole-trapnell-lab.github.io/projects/tophat/) and CuffLinks (cole-trapnell-lab.github.io/projects/cufflinks/), and expression data are presented as reads per kilobase of transcript per million reads mapped (RPKM). The RPKM values were normalized by adding 1 to all samples to calculate ratios even when RPKM = 0. The normalized RPKM readings of the experiment compared with control samples were used to calculate the positive and negative fold changes from their ratios. The differentially expressed mRNAs with a fold change of +1.5 or −1.5 were subjected to GSEA to identify the enriched pathways. Selected mRNAs in Fig. 6 were validated by qPCR. All primers were purchased from Qiagen.

**GSEA.** GSEA was performed using the CP: Canonical pathways of Molecular Signatures Database (MSigDB) of the Broad Institute (51). Enriched gene sets (pathways) were sorted based on the false discovery rate (FDR) values.

**IFN-Regulated Genes and Immune-Related Genes.** The databases of IFN-regulated genes and immune-related genes were obtained from www.interferome.org/interferome/home.jspx (52) and the ImmPort database, www.immport.org/immport-open/public/home/home, respectively.

**RNA-FISH and Immunofluorescence Microscopy.** RNA-FISH and immunofluorescence microscopy were performed as previously described (7).

**Statistical Analysis.** Statistical analyses were performed using two-sample, two-tailed *t* tests assuming equal variance. For statistical analysis of the M mRNA imaging study, a minimum of 50 cells was used for analysis in each condition. For all imaging studies, a one-sample Kolmogorov–Smirnov test was conducted. A normal distribution can be assumed for all populations ($P > 0.05$).

**ACKNOWLEDGMENTS.** We thank Xuewu Zhang for support in the crystallographic studies. This work was supported by NIH Grants R01AI125524-01 (to B.M.A.F., Y.M.C., A.G.-S., and K.W.L.) and R33 AI119304-01 (to B.M.A.F. and A.G.-S.), Cancer Prevention Research Institute of Texas Grants RP121003 and RP120718-P2/C2/P3 (to B.M.A.F. and Z.J.C.), and Welch Foundation Grant I-1532 (to Y.M.C.).

1. Palese P, Shaw ML (2007) Orthomyxoviridae: The virus and their replication. *Fields Virology*, eds Knipe DM, et al. (Lippincott Williams & Wilkins, Philadelphia), 5th Ed, pp 1647–1689.
2. Rossman JS, Jing X, Leser GP, Lamb RA (2010) Influenza virus M2 protein mediates ESCRT-independent membrane scission. *Cell* 142:902–913.
3. Tripathi S, et al. (2015) Meta- and orthogonal integration of influenza "OMICs" data defines a role for UBR4 in virus budding. *Cell Host Microbe* 18:723–735.
4. Gannagé M, et al. (2009) Matrix protein 2 of influenza A virus blocks autophagosome fusion with lysosomes. *Cell Host Microbe* 6:367–380.
5. Girard C, et al. (2012) Post-transcriptional spliceosomes are retained in nuclear speckles until splicing completion. *Nat Commun* 3:994.
6. Spector DL, Lamond AI (2011) Nuclear speckles. *Cold Spring Harb Perspect Biol* 3:a000646.
7. Mor A, et al. (2016) Influenza virus mRNA trafficking through host nuclear speckles. *Nat Microbiol*116069.
8. Thompson MG, et al. (2018) Co-regulatory activity of hnRNP K and NS1-BP in influenza and human mRNA splicing. *Nat Commun* 9:2407.
9. Tsai PL, et al. (2013) Cellular RNA binding proteins NS1-BP and hnRNP K regulate influenza A virus RNA splicing. *PLoS Pathog* 9:e1003460.
10. Valcárcel J, Portela A, Ortín J (1991) Regulated M1 mRNA splicing in influenza virus-infected cells. *J Gen Virol* 72:1301–1308.
11. Wahl MC, Will CL, Lührmann R (2009) The spliceosome: Design principles of a dynamic RNP machine. *Cell* 136:701–718.
12. Stogios PJ, Downs GS, Jauhal JJ, Nandra SK, Privé GG (2005) Sequence and structural analysis of BTB domain proteins. *Genome Biol* 6:R82.
13. Cansizoglu AE, Chook YM (2007) Conformational heterogeneity of karyopherin beta2 is segmental. *Structure* 15:1431–1441.
14. Dhanoa BS, Cogliati T, Satish AG, Bruford EA, Friedman JS (2013) Update on the Kelch-like (KLHL) gene family. *Hum Genomics* 7:13.
15. Wolff T, O'Neill RE, Palese P (1998) NS1-binding protein (NS1-BP): A novel human protein that interacts with the influenza A virus nonstructural NS1 protein is relocalized in the nuclei of infected cells. *J Virol* 72:7170–7180.
16. Perconti G, et al. (2007) The kelch protein NS1-BP interacts with alpha-enolase/MBP-1 and is involved in c-Myc gene transcriptional control. *Biochim Biophys Acta* 1773:1774–1785.
17. Dunham EE, Stevens EA, Glover E, Bradfield CA (2006) The aryl hydrocarbon receptor signaling pathway is modified through interactions with a Kelch protein. *Mol Pharmacol* 70:8–15.
18. Sasagawa K, et al. (2002) Identification of Nd1, a novel murine kelch family protein, involved in stabilization of actin filaments. *J Biol Chem* 277:44140–44146.
19. Chen HY, et al. (2015) KLHL39 suppresses colon cancer metastasis by blocking KLHL20-mediated PML and DAPK ubiquitination. *Oncogene* 34:5141–5151.
20. Gao R, et al. (2013) Heterogeneous nuclear ribonucleoprotein K (hnRNP-K) promotes tumor metastasis by induction of genes involved in extracellular matrix, cell movement, and angiogenesis. *J Biol Chem* 288:15046–15056.
21. Keppetipola NM, et al. (2016) Multiple determinants of splicing repression activity in the polypyrimidine tract binding proteins, PTBP1 and PTBP2. *RNA* 22:1172–1180.
22. Will CL, Lührmann R (2011) Spliceosome structure and function. *Cold Spring Harb Perspect Biol* 3:a003707.
23. Zhou Z, et al. (2000) The protein Aly links pre-messenger-RNA splicing to nuclear export in metazoans. *Nature* 407:401–405.
24. Kim DS, Hahn Y (2011) Identification of novel phosphorylation modification sites in human proteins that originated after the human-chimpanzee divergence. *Bioinformatics* 27:2494–2501.
25. Stogios PJ, Chen L, Privé GG (2007) Crystal structure of the BTB domain from the LRF/ZBTB7 transcriptional regulator. *Protein Sci* 16:336–342.
26. Murray JW, et al. (2009) Data from "Crystal structure of the BTB-BACK domains of human KLHL11." RCSB Protein Data Bank. Available at https://www.rcsb.org/structure/3I3N. Accessed August 4, 2009.
27. Evans SE, et al. (2014) The ansamycin antibiotic, rifamycin SV, inhibits BCL6 transcriptional repression and forms a complex with the BCL6-BTB/POZ domain. *PLoS One* 9:e90889.
28. Canning P, et al. (2013) Structural basis for Cul3 protein assembly with the BTB-Kelch family of E3 ubiquitin ligases. *J Biol Chem* 288:7803–7814, and correction (2013) 388:28304.
29. Kim JH, Hahm B, Kim YK, Choi M, Jang SK (2000) Protein-protein interaction among hnRNPs shuttling between nucleus and cytoplasm. *J Mol Biol* 298:395–405.
30. Fukutomi T, Takagi K, Mizushima T, Ohuchi N, Yamamoto M (2014) Kinetic, thermodynamic, and structural characterizations of the association between Nrf2-DLGex degron and Keap1. *Mol Cell Biol* 34:832–846.
31. Lo SC, Li X, Henzl MT, Beamer LJ, Hannink M (2006) Structure of the Keap1:Nrf2 interface provides mechanistic insight into Nrf2 signaling. *EMBO J* 25:3605–3617.
32. Schumacher FR, Sorrell FJ, Alessi DR, Bullock AN, Kurz T (2014) Structural and biochemical characterization of the KLHL3-WNK kinase interaction important in blood pressure regulation. *Biochem J* 460:237–246.
33. Engelhardt OG, Fodor E (2006) Functional association between viral and cellular transcription during influenza virus infection. *Rev Med Virol* 16:329–345.
34. Engelhardt OG, Smith M, Fodor E (2005) Association of the influenza A virus RNA-dependent RNA polymerase with cellular RNA polymerase II. *J Virol* 79:5812–5818.
35. Shih SR, Nemeroff ME, Krug RM (1995) The choice of alternative 5′ splice sites in influenza virus M1 mRNA is regulated by the viral polymerase complex. *Proc Natl Acad Sci USA* 92:6324–6328.
36. David CJ, Boyne AR, Millhouse SR, Manley JL (2011) The RNA polymerase II C-terminal domain promotes splicing activation through recruitment of a U2AF65-Prp19 complex. *Genes Dev* 25:972–983.
37. Wongpalee SP, et al. (2016) Large-scale remodeling of a repressed exon ribonucleoprotein to an exon definition complex active for splicing. *eLife* 5:e19743.
38. Pereira CF, Read EKC, Wise HM, Amorim MJ, Digard P (2017) Influenza A virus NS1 protein promotes efficient nuclear export of unspliced viral M1 mRNA. *J Virol* 91:e00528-17.
39. Heath CG, Viphakone N, Wilson SA (2016) The role of TREX in gene expression and disease. *Biochem J* 473:2911–2935.
40. Howard JM, Sanford JR (2015) The RNAissance family: SR proteins as multifaceted regulators of gene expression. *Wiley Interdiscip Rev RNA* 6:93–110.
41. Burotto M, Chiou VL, Lee JM, Kohn EC (2014) The MAPK pathway across different malignancies: A new perspective. *Cancer* 120:3446–3456.
42. Dovizio M, Sacco A, Patrignani P (2017) Curbing tumorigenesis and malignant progression through the pharmacological control of the wound healing process. *Vascul Pharmacol* 89:1–11.
43. Minor W, Cymborowski M, Otwinowski Z, Chruszcz M (2006) HKL-3000: The integration of data reduction and structure solution–From diffraction images to an initial model in minutes. *Acta Crystallogr D Biol Crystallogr* 62:859–866.
44. Adams PD, et al. (2010) PHENIX: A comprehensive Python-based system for macromolecular structure solution. *Acta Crystallogr D Biol Crystallogr* 66:213–221.
45. McCoy AJ (2007) Solving structures of protein complexes by molecular replacement with Phaser. *Acta Crystallogr D Biol Crystallogr* 63:32–41.
46. Emsley P, Lohkamp B, Scott WG, Cowtan K (2010) Features and development of Coot. *Acta Crystallogr D Biol Crystallogr* 66:486–501.
47. Schuck P (2000) Size-distribution analysis of macromolecules by sedimentation velocity ultracentrifugation and Lamm equation modeling. *Biophys J* 78:1606–1619.
48. Brautigam CA (2015) Calculations and publication-quality illustrations for analytical ultracentrifugation data. *Methods Enzymol* 562:109–133.
49. Kuss-Duerkop SK, et al. (2017) Influenza virus differentially activates mTORC1 and mTORC2 signaling to maximize late stage replication. *PLoS Pathog* 13:e1006635.
50. Andrews S (2010) FastQC: A quality control tool for high throughput sequence data. Available at www.bioinformatics.babraham.ac.uk/projects/fastqc. Accessed January 7, 2018.
51. Subramanian A, et al. (2005) Gene set enrichment analysis: A knowledge-based approach for interpreting genome-wide expression profiles. *Proc Natl Acad Sci USA* 102:15545–15550.
52. Rusinova I, et al. (2013) Interferome v2.0: An updated database of annotated interferon-regulated genes. *Nucleic Acids Res* 41:D1040–D1046.